

## Supporting Information

### **Stable High-Efficiency Monolithic All-Perovskite Tandem Solar Cells Enabled by a Natural Reactive Oxygen Species Scavenger.**

*Ruitian Sun,<sup>a</sup> Pengshuai Wang,<sup>a</sup> Lin Zhang,<sup>a</sup> Weijun Liu,<sup>b</sup> Yanjie Wen,<sup>b</sup> Fan Li,<sup>b</sup> Zhizhong Ge,<sup>a</sup> Liang Qiao,<sup>a</sup> Tao Wang,<sup>a</sup> Tianshi Ye,<sup>a</sup> Peijun Ji,<sup>a</sup> Xudong Yang<sup>\*a,b,c,d</sup>*

*<sup>a</sup>State Key Laboratory of Metal Matrix Composites, Shanghai Jiao Tong University, Shanghai 200240, China.*

*<sup>b</sup>Shenzhen Solaeon Technology Co., Ltd. Shenzhen 518000, China*

*<sup>c</sup>Center of Hydrogen Science, School of Materials Science and Engineering, Shanghai Jiao Tong University, Shanghai, 200240, China.*

*<sup>d</sup>Innovation Center for Future Materials, Zhangjiang Institute for Advanced Study, Shanghai Jiao Tong University, Shanghai, 201210, China.*

*\*Corresponding author. Email: yang.xudong@sjtu.edu.cn*

## Supplementary Note 1

Density functional theory (DFT) calculations were performed using the Vienna ab initio simulation package (VASP)<sup>[1,2]</sup> with the standard frozen-core projector augmented-wave (PAW) method<sup>[3,4]</sup>. The exchange-correlation effects were approximated by the generalized gradient approximation (GGA) utilizing the Perdew–Burke–Ernzerhof (PBE) functional.<sup>[5]</sup> The kinetic energy cut-off for the plane wave basis was set to 400 eV and a 7x7x7 Gamma-centered k-point mesh was used. The geometric structure was completely relaxed until the electron relaxation convergence criterion dropped below 10<sup>-5</sup> eV/atom and the remaining force was less than 0.02 eV/Å. Additionally, the Grimme DFT-D3 method has been considered to further describe the van der Waals interactions.<sup>[6]</sup>

The binding energies for various bulk materials (including FAPbI<sub>3</sub>, FASnI<sub>3</sub>, CNL-PbI<sub>2</sub> and CNL-SnI<sub>2</sub>) were calculated as follows. For Pb-based compounds, the binding energy  $\Delta E_{\text{FAPbI}_3}$  is defined by the equation  $\Delta E_{\text{FAPbI}_3} = E_{\text{FAPbI}_3} - E_{\text{PbI}_2} - E_{\text{FAI}}$ , where  $E_{\text{FAPbI}_3}$ ,  $E_{\text{PbI}_2}$  and  $E_{\text{FAI}}$  are calculated total energies of bulk FAPbI<sub>3</sub>, PbI<sub>2</sub> and crystalline FAI in cubic, trigonal and monoclinic symmetry, respectively.<sup>[7]</sup>  $\Delta E_{\text{CNL-PbI}_2} = E_{\text{CNL-PbI}_2} - E_{\text{PbI}_2} - E_{\text{CNL}}$ , where  $E_{\text{CNL-PbI}_2}$ ,  $E_{\text{PbI}_2}$  and  $E_{\text{CNL}}$  are calculated total energies of bulk CNL-PbI<sub>2</sub>, PbI<sub>2</sub> and gas-phase CNL. The calculations for Sn-based compounds is similarly. The visualization of electrostatic potential (ESP) and crystal structures was facilitated using

VMD<sup>[8]</sup> and VESTA software, respectively.<sup>[9]</sup>

## Supplementary Note 2

The decay curves were fitted using the bi-exponential equation:

$$Y=A_1 \exp\left(\frac{-t}{\tau_1}\right)+A_2 \exp\left(\frac{-t}{\tau_2}\right)$$

where fast ( $\tau_1$ ) and slow ( $\tau_2$ ) decay components correspond to non-radiative and radiative recombination, respectively.<sup>[10]</sup> The fitting parameters were presented in Table S3 (Supporting Information) and the average carrier lifetime was calculated using the equation:<sup>[11]</sup>

$$\tau_{average}=\frac{A_1 \tau_1^2+A_2 \tau_2^2}{A_1 \tau_1+A_2 \tau_2}$$

## Supplementary Note 3

The trap density of the perovskite film was determined using the equation:

$$N_t=\frac{2\varepsilon \varepsilon_0 V_{TFL}}{eL^2}$$

where  $N_t$  represents the trap density ( $\text{cm}^{-3}$ ),  $\varepsilon_0$  denotes the vacuum dielectric constant ( $8.85 \times 10^{-12} \text{ F m}^{-1}$ ),  $\varepsilon$  represents the relative dielectric constant of the perovskite ( $\sim 32$ ),  $e$  is the elementary electric charge ( $1.6 \times 10^{-19} \text{ C}$ ),  $L$  represents the perovskite film thickness ( $\sim 900 \text{ nm}$ ), and  $V_{TFL}$  represents the trap-filled limit voltage, which can be deduced from SCLC spectra (Figure 2i). The  $V_{TFL}$  of the control and CNL devices were 0.345 V and 0.17 V, respectively.

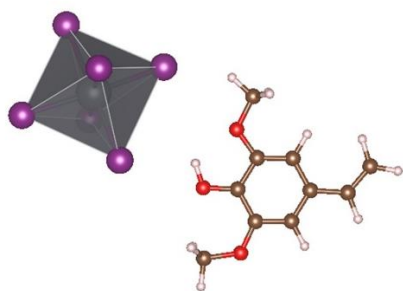
#### **Supplementary Note 4**

The ideality factor  $n$  is a critical parameter that provides insight into the recombination mechanisms within the solar cell. The ideality factor can be determined using the following equation:

$$\frac{d(V_{oc})}{d(\ln L)} = n \frac{k_B T}{q}$$

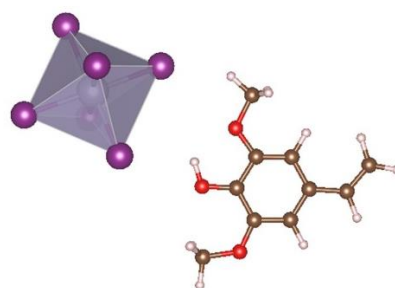
where  $L$  represents the light intensity,  $k_B$  represents Boltzmann constant (approximately  $1.38 \times 10^{-23}$  J/K),  $T$  is the absolute temperature (in Kelvin),  $q$  is the elementary electric charge ( $1.6 \times 10^{-19}$  C).

a



CNL-PbI<sub>2</sub>

b



CNL-SnI<sub>2</sub>

**Figure S1.** Schematic of coordination between CNL and PbI<sub>2</sub>/SnI<sub>2</sub>.

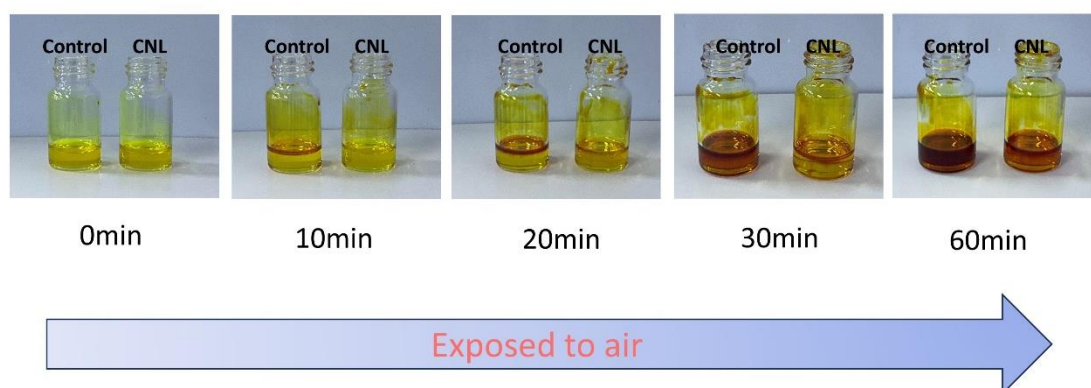


**Figure S2.** Photographs of control and CNL NBG  $(\text{FASnI}_3)_{0.6}(\text{MAPbI}_3)_{0.4}$  perovskite precursor solutions exposed to ambient air for varying durations.

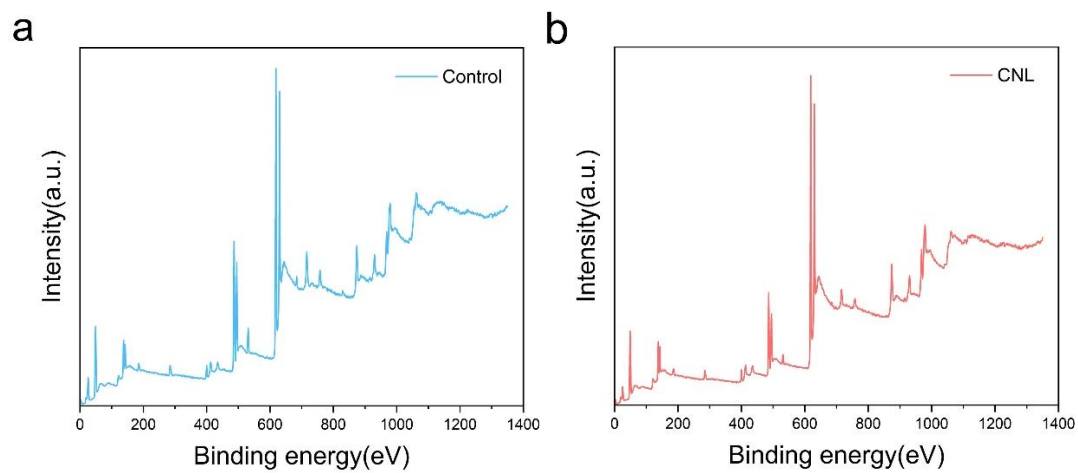


**Figure S3.** Full scan of XPS spectra of the **a**, control and **b**, CNL perovskite films.

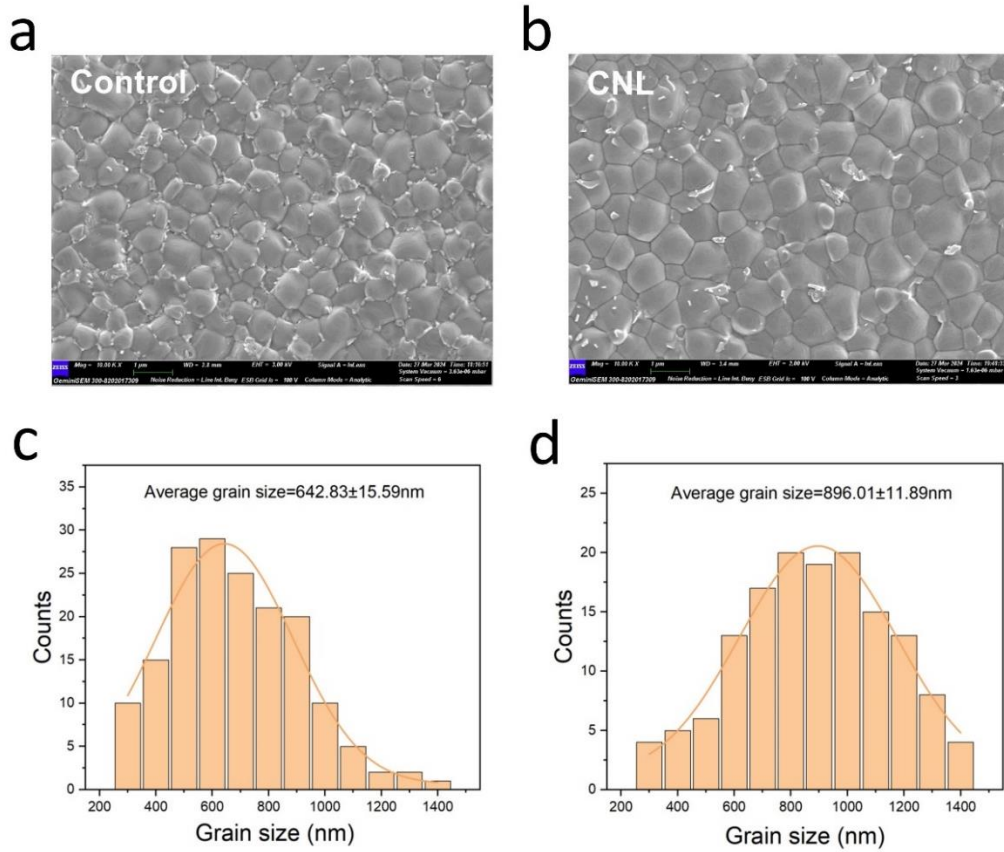


**Figure S4.** Top-view SEM images and grain size distributions of the **a**, control and **b**, CNL perovskite films.



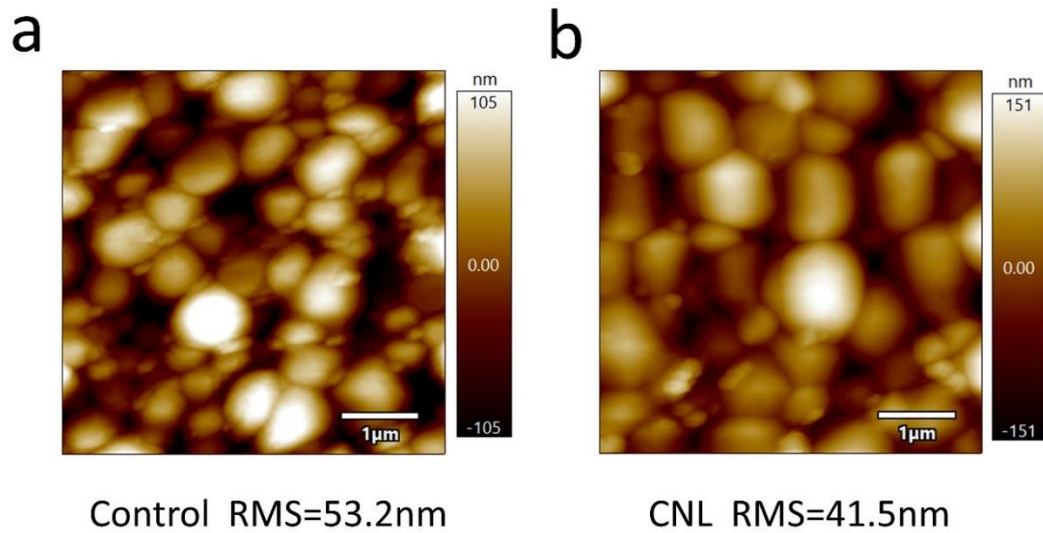


**Figure S5.** AFM images of the **a**, control and **b**, CNL perovskite films.

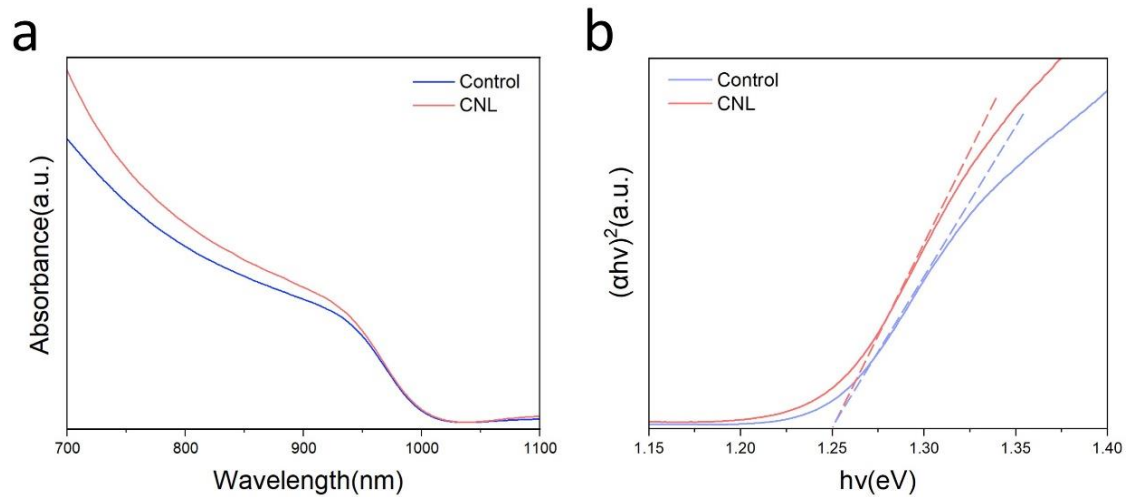


**Figure S6. a**, UV-Vis-NIR absorption spectra of the control and CNL perovskite films **b**, Tauc plots of the control and CNL perovskite films.

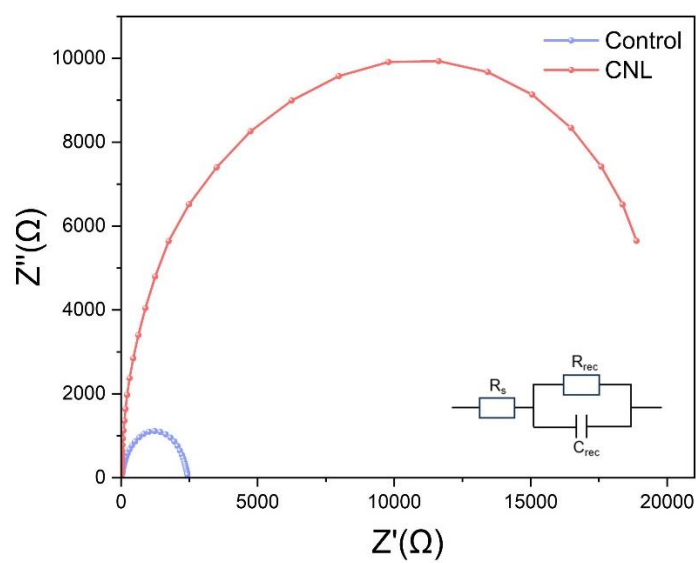


**Figure S7.** Electronic impedance spectroscopy (EIS) plots of the control and CNL NBG single junction PSCs. The inset shows the equivalent circuit diagram of EIS measurements.

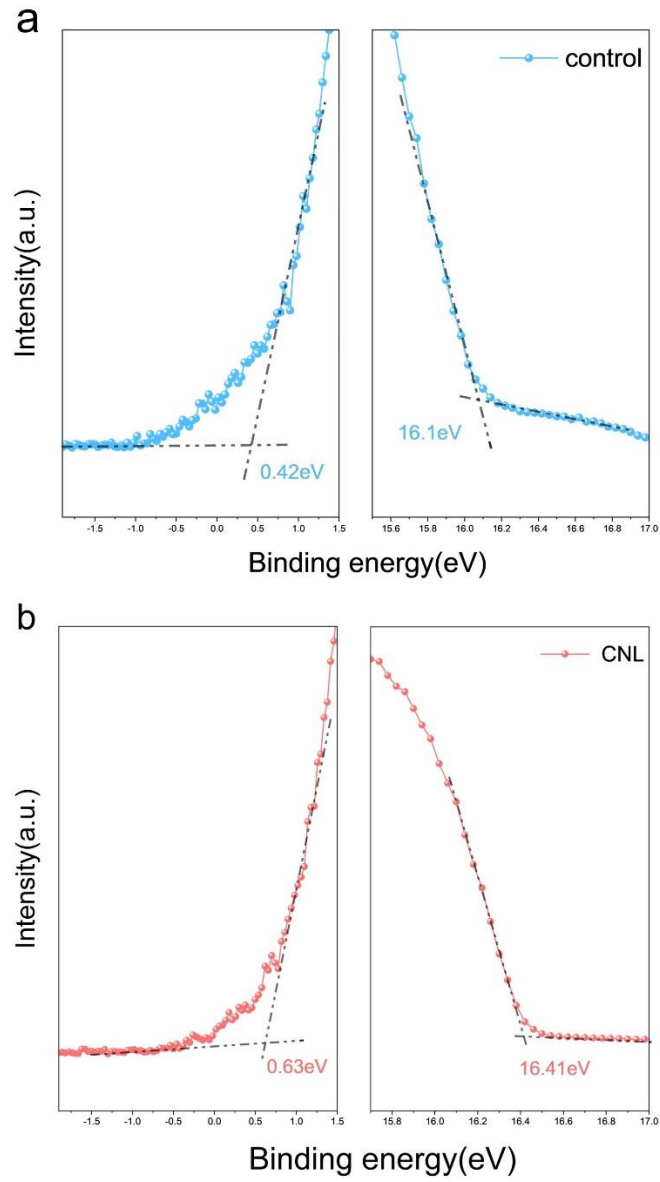


**Figure S8.** UPS spectra of the **a**, control and **b**, CNL perovskite films.

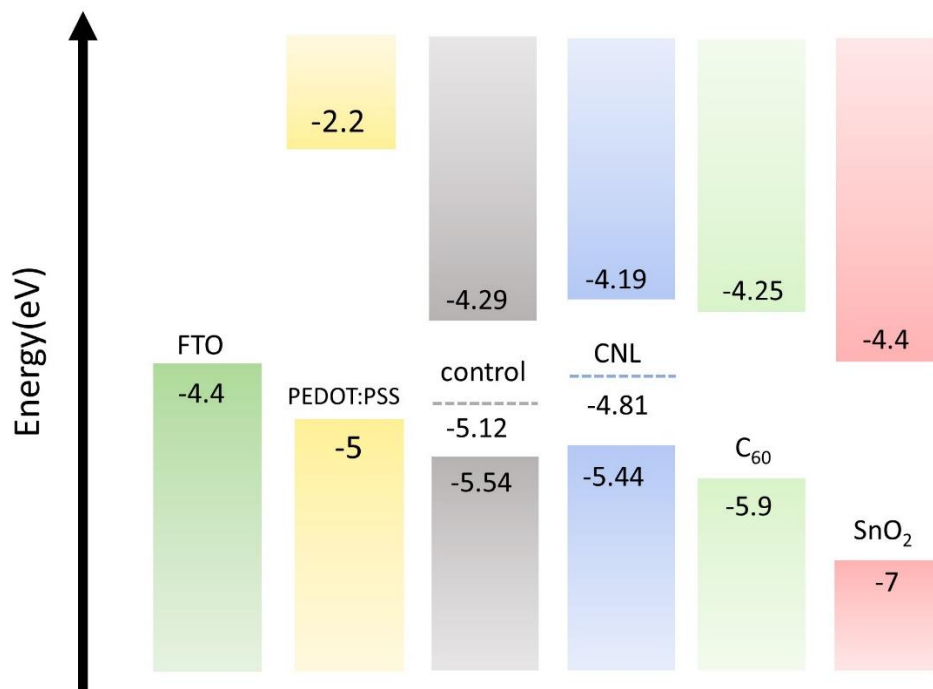


**Figure S9.** Energy level diagram of the devices based on mixed Sn-Pb perovskites.

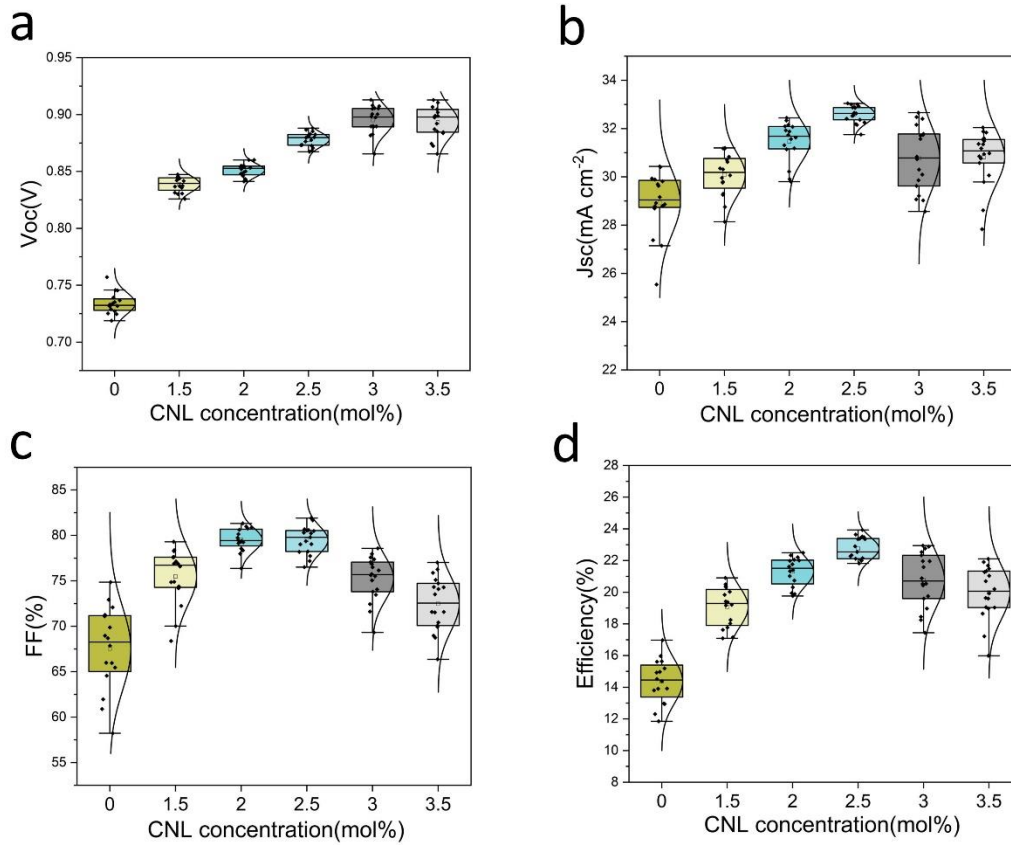


**Figure S10.** Statistics of J-V parameters for single junction NBG PSCs without or with different concentrations of CNL (1.5, 2, 2.5, 3 and 3.5 mol%, relative to MAI+FAI in perovskite) **a**,  $V_{oc}$ ; **b**,  $J_{sc}$ ; **c**, FF; **d**, Efficiency.

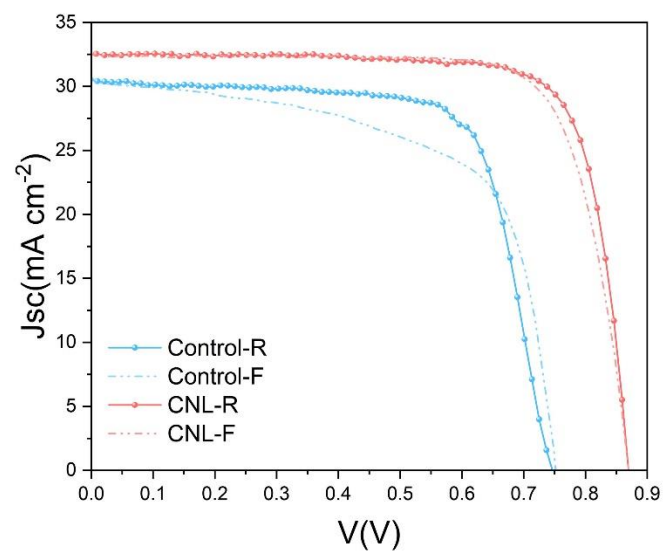


**Figure S11.** J-V curves of the champion control and CNL single junction NBG perovskite solar cells under reverse (R) and forward (F) voltage scan (aperture area of  $1.035 \text{ cm}^2$ ).

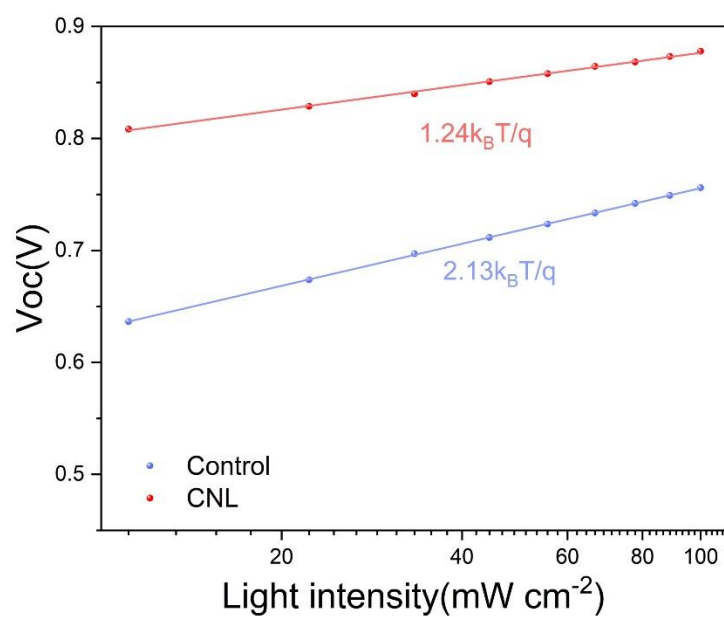


**Figure S12.** Fitting curves of light intensity-dependent  $V_{oc}$  measurements for control and CNL single junction NBG perovskite solar cells.



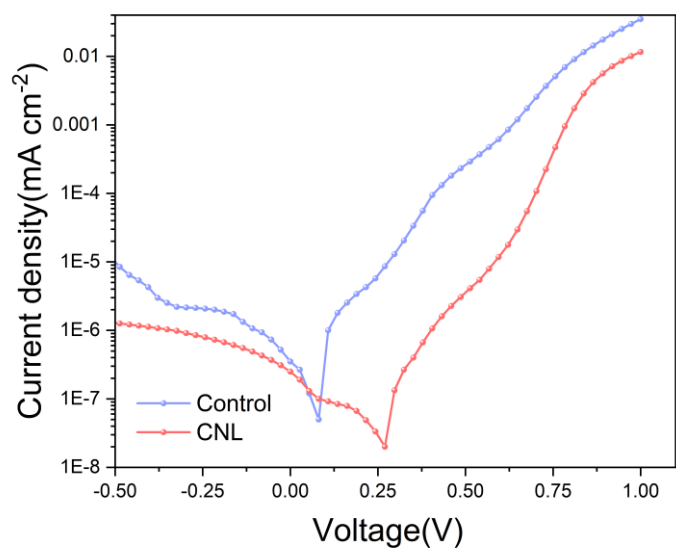


**Figure S13.** Dark J-V curves of the control and CNL single junction NBG perovskite solar cells.

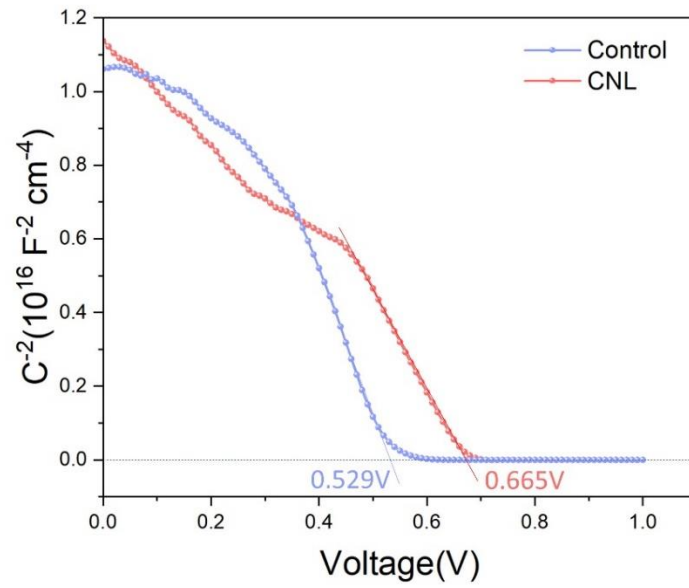


**Figure S14.** Curves of Mott-Schottky (M-S) measurements of the control and CNL single junction NBG perovskite solar cells.

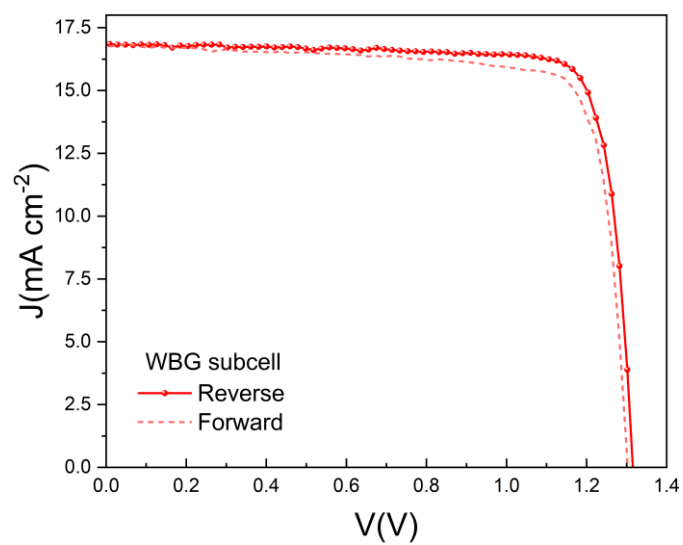


**Figure S15.** J-V curves of the champion single junction WBG perovskite solar cell under reverse (R) and forward (F) voltage scan (aperture area of 0.077 cm<sup>2</sup>).

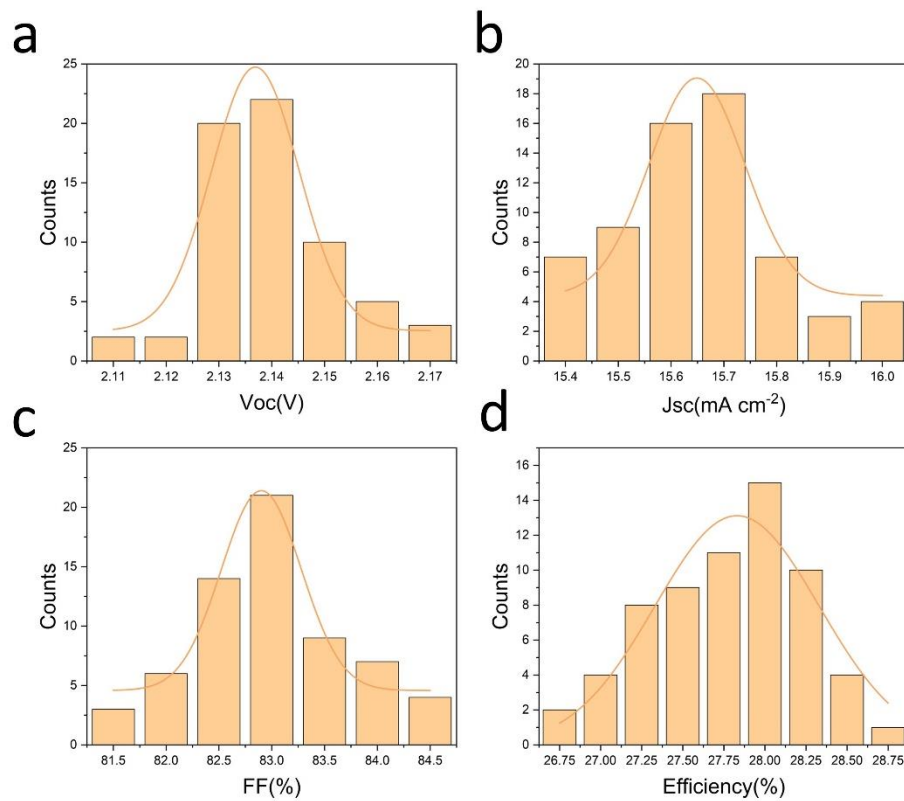


**Figure S16.** Photovoltaic performance distributions of 64 monolithic all-perovskite tandem solar cells **a**,  $V_{oc}$ ; **b**,  $J_{sc}$ ; **c**, FF; **d**, Efficiency.

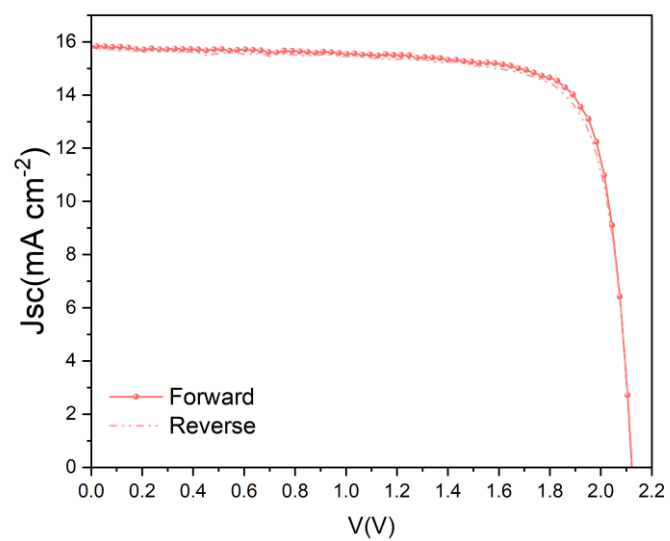


**Figure S17.** J-V curves of the champion monolithic all-perovskite tandem solar cells under reverse (R) and forward (F) voltage scan (aperture area of 1.035 cm<sup>2</sup>).

### 1. Testing Method (Code and Name) for This Test

IEC 60904-1: 2020 Photovoltaic devices- Part 1: Measurement of photovoltaic current-voltage characteristics.

### 2. Measurement Standards Used in This Test

Measurement Standards Used in This Test					
Name	Number	Measuring Range	Uncertainty or Accuracy Class or Maximum Permissible Error	Name of Traceability Institution/Certificate No.	Due Date
SourceMeter	10807C0087 8-2	DCI: (-10 $\mu$ A-1A); DCV: (20mV~20V)	Measure: DCV: $U_{rel}=0.05\%,k=2$ ; DCI: $U_{rel}=0.05\%,k=2$ Output: DCV: $U_{rel}=0.05\%,k=2$ ; DCI: $U_{rel}=0.05\%,k=2$	Fujian Metrology Institute/ 23D2-02429	2024-04-16
Solar Simulator	2014-017	(300~1200) nm; (800~ 1200) W/m <sup>2</sup>	Spectral Match: (300~360) nm: $U_{rel}=8.0\% (k=2)$ ;(360~ 1200) nm: $U_{rel}=6.2\%$ ( $k=2$ );Irradiance Ratio: $U_{rel}=1.2\% (k=2)$	Fujian Metrology Institute/ 23Q2-00526	2024-06-13
WPVS Reference Solar Cell	015-2014	(300~1200) nm	$U=1.3\% (k=2)$	National Institute of Metrology, China/GXgf2023-01245	2025-03-29
Digital Thermometer	15-B	(15~65) $^{\circ}$ C	$U=0.1\% (k=2)$	Fujian Metrology Institute/23B2-07940	2024-06-18

### 3. Test Location

Room 108, Building 4, MinHou Scientific Research Base

### 4. Environmental Condition

Temperature: 25.5 $^{\circ}$ C; Relative Humidity: 37%

### 5. Standard Test Condition (STC):

Total Irradiance: 1000 W/m<sup>2</sup>

Temperature for DUT: 25.0 °C

Spectral Distribution: AM1.5G

### 6. Measurement Data under STC

Scan Direction	$I_{sc}$ (mA)	$V_{oc}$ (V)	$I_{MPP}$ (mA)	$V_{MPP}$ (V)	$P_{MPP}$ (mW)	FF (%)	$\eta$ (%)	Area (cm <sup>2</sup> )
Forward	1.222	2.138	1.140	1.863	2.124	81.30	27.60	
Reverse	1.223	2.136	1.158	1.893	2.192	83.91	28.48	

### 7. I-V & P-V Characteristic Curves under STC

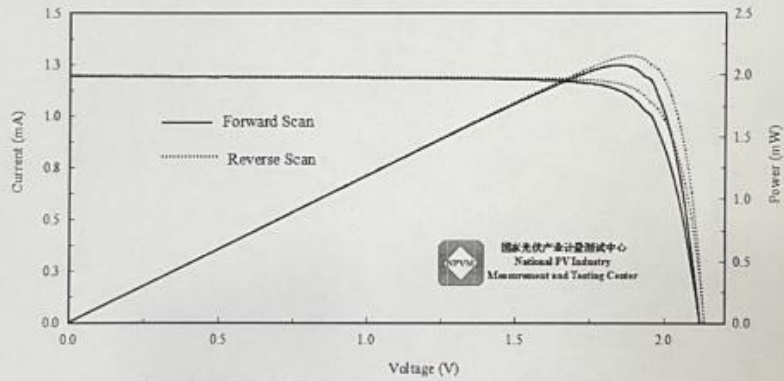


Figure 1. I-V and P-V characteristic curves of cell under STC

### 8. Pictures of the Measured Sample

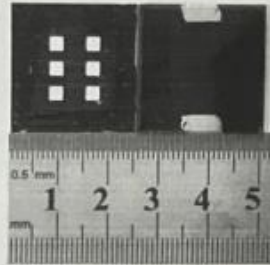


Figure 2. Obverse side of the sample and mask used during test

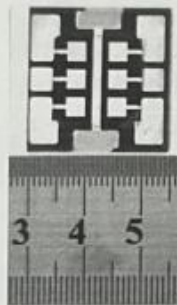


Figure 3. Reverse side of the measured sample

Test by: 陈彩云 (Chen Caiyun)

Checked by: 何翔 (He Xiang)

Approved by: 李健生 (Li Jiansheng)

Date: 2024.03.15

**Figure S18.** Certification report for an encapsulated all-perovskite tandem solar cell based on a CNL NBG subcell by Chinese National PV Industry Measurement and Testing Center (NPVM).



## Supplemental Tables

**Table S1.** Summary of the efficiency and operation stability of the recent reported NBG PSCs and all-perovskite TSCs

PCE-NBG(%)	PCE-TSC(%)	MPPT-TSC	Ref
20.74	25.6	T88-500h	Tan et al. <i>Nat. Energy</i> , <b>2020</b> , 5, 870-880.
22.2	26.7	T90-600h	Tan et al. <i>Nature</i> , <b>2022</b> , 603, 73-78.
22.2	25.5	T80-1500h	Zhu et al. <i>Nat. Energy</i> , <b>2022</b> , 7, 642-651.
21.51	25.05	T90-450h	Li et al. <i>Nat. Energy</i> , <b>2022</b> , 7, 744-753.
21.5	26.29	T86-500h	Sargent et al. <i>Nature</i> , <b>2023</b> , 613, 676-681.
23.24	26.3	T80-301h	Zhao et al. <i>Nat. Energy</i> , <b>2023</b> , 8, 714-724.
23.8	28	T90-600h	Tan et al. <i>Nature</i> , <b>2023</b> , 620, 994-1000.
21.72	27.34	/	Ke et al. <i>Nature</i> , <b>2023</b> , 624,69-73.
22.58	26.33	T88-1000h	Wang et al. <i>Energy Environ. Sci.</i> <b>2024</b> , 17, 2512-2520.
21.65	26.96	T80-370h	Ning et al. <i>Nat. Energy</i> , <b>2024</b> , 9, 298-307.
23.11	27.35	/	Ke et al. <i>Nat. Commun.</i> <b>2024</b> , 15, 2324.
21.88	27.81	T80-292h	Zhao et al. <i>Sci. Adv.</i> <b>2024</b> , 10, 16
22.7	27.8	T90>1000h	Yan et al. <i>Joule</i> , <b>2024</b>
23.7	28.48	T90-750h	This work.

**Table S2.** Photovoltaic parameters of the champion WBG subcell, NBG subcell and tandem solar cell (aperture area of 0.077 cm<sup>2</sup>).

	Scan Direction	J <sub>sc</sub> (mA cm <sup>-2</sup> )	V <sub>oc</sub> (V)	FF (%)	PCE (%)
NBG (control)	Reverse	30.42	0.757	74.8	17.22
	Forward	30.4	0.751	68.64	15.67
NBG (CNL)	Reverse	32.85	0.883	81.7	23.7
	Forward	32.86	0.888	80.08	23.38
WBG	Reverse	16.9	1.314	83.15	18.46
	Forward	16.79	1.301	80.81	17.65
Tandem (control)	Reverse	14.32	1.996	78.83	22.55
	Forward	14.33	1.999	74.13	21.23
Tandem (CNL)	Reverse	15.77	2.153	84.58	28.71
	Forward	15.77	2.156	83.1	28.25
	Stabilized	—	—	—	28.56

**Table S3.** Photovoltaic parameters of the champion NBG and tandem perovskite solar cell (aperture area of 1.035 cm<sup>2</sup>).

	Scan Direction	Jsc (mA cm <sup>-2</sup> )	Voc (V)	FF (%)	PCE (%)
NBG (control)	Reverse	30.4	0.752	71.3	16.30
	Forward	30.38	0.752	63.63	14.54
NBG (CNL)	Reverse	32.5	0.869	78.18	22.08
	Forward	32.37	0.869	76.31	21.47
Tandem	Reverse	15.8	2.12	81.21	27.2
	Forward	15.76	2.121	79.51	26.57

**Table S4.** PL decay lifetimes of control and CNL perovskite films.  $\tau_1$  and  $\tau_2$  correspond to the fast and slow decay components, respectively.

	$\tau_1(\text{ns})$	$A_1$	$\tau_2(\text{ns})$	$A_2$	$\tau_{\text{average}}(\text{ns})$
Control	8.547	0.823	153.8	0.53	123.91
CNL	6.538	0.53	417.52	0.434	409.81

## REFERENCES

- [1] G. Kresse, J. Hafner, *Phys. Rev. B*, 1993, **47**, 558.
- [2] G. Kresse, J. Furthmuller, *Phys. Rev. B*, 1996, **54**, 11169.
- [3] P. E. Blöchl, *Phys. Rev. B*, 1994, **50**, 17953.
- [4] G. Kresse, D. Joubert. *Phys. Rev. B*, 1999, **59**, 1758.
- [5] J. P. Perdew, K. Burke, M. Ernzerhof, *Phys. Rev. Lett.*, 1996, **77**, 3865.
- [6] S. Grimme, J. Antony, S. Ehrlich, H. Krieg, *J. Chem. Phys.*, 2010, **132**, 154104.
- [7] A. A. Petrov, E. A. Goodilin, A. B. Tarasov, V. A. Lazarenko, P. V. Dorovatovskii, V. N. Khrustalev, *Acta Cryst.*, 2017, **73**, 569-572.
- [8] W. Humphrey, A. Dalke, K. Schulten, *J. Molec. Graphics*, 1996, **14**, 33.
- [9] K. Momma, F. Izumi, *J. Appl. Cryst.*, 2011, **44**, 1272-1276.
- [10] M. Jeong, I. W. Choi, E. M. Go, Y. Cho, M. Kim, B. Lee, S. Jeong, Y. Jo, H. W. Choi, J. Lee, J. H. Bae, S. K. Kwak, D. S. Kim, C. Yang, *Science*, 2020, **369**, 1615-1620.
- [11] J. Zhou, S. Fu, S. Zhou, L. Huang, C. Wang, H. Guan, D. Pu, H. Cui, C. Wang, T. Wang, W. Meng, G. Fang, W. Ke, *Nat. Commun.*, 2024, **15**, 2324.